

# Molecular Mobility, Ion Mobility, and Mobile Ion Concentration in Poly(ethylene oxide)-Based Polyurethane Ionomers

Daniel Fragiadakis, Shichen Dou, Ralph H. Colby, and James Runt\*

Department of Materials Science and Engineering and Materials Research Institute, The Pennsylvania State University, University Park, Pennsylvania 16802

Received February 4, 2008; Revised Manuscript Received April 28, 2008

**ABSTRACT:** The segmental and local chain dynamics as well as the transport of  $\text{Na}^+$  and  $\text{Li}^+$  cations in a series of model poly(ethylene oxide)-based polyurethane ionomers is investigated using dielectric relaxation spectroscopy. A physical model of electrode polarization is employed to separately determine mobile ion concentration and ion mobility in these single-ion conductors. A model including unpaired ions, separated ion pairs, and contact ion pairs is used to reconcile the very small fraction of free ions obtained using the electrode polarization model with those of previous studies of ion association in polyether-based single-ion conducting and salt-containing systems.

## 1. Introduction

Polymer electrolytes play a critical role in energy storage devices such as lithium batteries and fuel cells, acting as a medium for ion transport between the active components of the device. Despite the practical importance of these materials and after several decades of research, many aspects of ion transport through polymers are incompletely understood, and progress in the field remains largely empirical.<sup>1–4</sup>

Currently used polymer electrolytes are so-called “gel” electrolytes, polymers containing a large amount of liquid electrolyte (solvent plus lithium salt) through which ion transport occurs. A major challenge is the replacement of these materials with solid, solvent-free polymer electrolytes, either polymer–salt complexes where both anions and cations are mobile or single-ion conductors with anions fixed to the polymer chains. However, the low conductivity of such materials compared to gels has proven a major obstacle to their commercial application.<sup>4</sup>

Both experimental studies and molecular dynamics simulations<sup>5–7</sup> have provided valuable information on the basic mechanism of charge transport in polyether-based systems. It is generally agreed that conducting cations are complexed with several ether oxygen atoms (4–6 for  $\text{Li}^+$  ions). Therefore, ion mobility is strongly coupled to segmental mobility and controlled by the glass transition temperature of the polymer.

Ions in polymer electrolytes are able to associate into pairs and larger aggregates, and ionic conductivity is determined both by the number of mobile charge carriers and by their mobility. A number of different approaches have been taken to separate conductivity into the contributions from mobile ion concentration and ion mobility; the results however are not conclusive. Many experimental studies employing vibrational spectroscopy,<sup>8–10</sup> pulsed-field gradient NMR,<sup>11</sup> and radiotracer diffusion<sup>12–14</sup> as well as molecular dynamics simulations<sup>5</sup> indicate only a modest degree of ion association, most ions being free and contributing to conduction. On the other hand, recent dielectric spectroscopy studies, employing modeling of electrode polarization, suggest that the vast majority of ions exist in a bound state, with a very small fraction contributing to dc conduction.<sup>15–17</sup> Such discrepancies indicate that different definitions of “free” or “mobile” ions apply to different experimental techniques, and a more precise description of

various ion association states is needed in order to attempt to reconcile all results.

This paper is part of our continuing investigation of ion transport in model polymer systems.<sup>15,16</sup> The materials studied here are PEO-based polyurethane single-ion ( $\text{Li}^+$  or  $\text{Na}^+$ ) conductors, with the anions covalently bound to the polymer chains. The conduction measured is thus due exclusively to cation motion, the conduction process of interest for practical applications, and analysis is not complicated by the presence of mobile anions which often dominate the conductivity of salt-containing polyethers because the cations are coordinated with multiple ether oxygens. Unlike previously studied ethylene oxide-based polyurethane ionomers,<sup>18–20</sup> the ionomers studied here are amorphous, single-phase materials with no ion clustering of the type typically observed in ionomers, perhaps making the interpretation of the conductivity parameters more straightforward.

## 2. Experimental Section

**2.1. Sample Preparation.** Samples were synthesized in two steps. Initially, dimethyl 5-sulfoisophthalate sodium salt was chain-extended using poly(ethylene glycol) ( $M_n = 600$  g/mol) to form a prepolymer. Appropriate amounts of dry dimethyl 5-sulfoisophthalate sodium salt (DM5SIS), poly(ethylene glycol) (PEG600,  $M_n = 600$  g/mol), and the catalyst dibutyltin oxide (0.05 wt %) were placed in a glass reactor maintained under an argon atmosphere. The molar ratio of DM5SIS to PEG600 was 1:2. The mixture was stirred mechanically, and the temperature of the reaction was maintained at 170 for 3 h followed by 190 for 4 h. Vacuum was applied to remove low molecular weight species. The product (DiPEG600-5SISNa) was precipitated from acetone solution using ethyl ether.

The final polymer was formed by polycondensation of the prepolymer with isophorone diisocyanate. 30 g of DiPEG600-5SISNa and dry isophorone diisocyanate (molar ratio 1:1) were dissolved in 80 mL of purified DMF in a reactor maintained under an argon atmosphere. The temperature of reaction was kept between 60 and 70 °C for 12 h. 0.2 mL of ethylene glycol (chain extender) was then added, and the reaction was continued for an additional 12 h. The polyurethane ionomer was precipitated from acetone solution using ethyl ether and dried at 100 °C under vacuum for 12 h. The chemical structure of the resulting material is shown in Figure 1. It consists of poly(ethylene oxide) segments of molecular weight 600 linked together alternately by the ion-containing

\* Corresponding author: e-mail runt@matse.psu.edu.

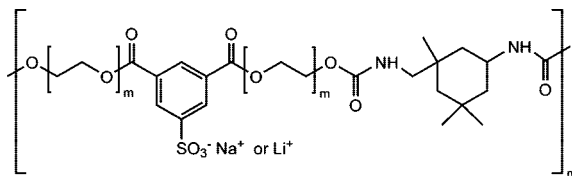


**Figure 1.** Chemical structure of the polyurethane ionomers under investigation.

**Table 1.** Number-Average Molecular Weight  $M_n$ , Calorimetric Glass Transition Temperature  $T_g$ , and Stoichiometric Cation Concentration  $p_0$  for the Materials under Investigation (Uncertainty for  $T_g$  Is  $\pm 2$  K)

sample	$M_n$ [g/mol]	$T_g$ [K]	$p_0$ [cm $^{-3}$ ]
PU $^-$ Li $^+$	17 000	253	$3 \times 10^{20}$
PU $^-$ Na $^+$	11 000	257	$3 \times 10^{20}$

sulfonated isophthalate group and by the substituted methylene cyclohexane ring connected by two urethane linkages.

A lithium-containing ionomer was prepared from the sodium-containing sample by dialysis after exposure to an excess of LiCl in water. The sodium and lithium containing ionomers will be referred to in the following as PU $^-$ Na $^+$  and PU $^-$ Li $^+$ , respectively.  $^1\text{H}$  NMR was used to confirm the structure of the polymer in Figure 1 and determine the number-average molecular weights shown in Table 1.

**2.2. Experimental Techniques. Small-Angle X-ray Scattering.** SAXS measurements were performed using a Molecular Metrology instrument equipped with a Cu target ( $\lambda = 1.542$  Å) and a two-dimensional area proportional counter. A silver behenate standard was used to calibrate the scattering vector. Scattering data were collected for 3 h.

**Thermal Characterization.** Glass transition temperatures ( $T_g$ ) were determined using a TA Q100 differential scanning calorimeter (DSC). Sample weights were  $\sim 15$  mg. Samples were held at 393 K for 3 min, then cooled to 198 K at 10 K/min, and subsequently heated to 393 K at 10 K/min.  $T_g$  was obtained from the heating scan as the midpoint of the heat capacity transition.

**Dielectric Relaxation Spectroscopy.** Samples for DRS measurements were placed onto a brass electrode and dried in a vacuum oven at 353 K for 24 h, after which a second brass electrode was placed on top of the sample. A Teflon spacer was used to control the sample thickness at 200  $\mu\text{m}$ . A Novocontrol GmbH Concept 40 broadband dielectric spectrometer was used to measure the dielectric permittivity. Frequency sweeps were performed isothermally from 10 MHz to 0.01 Hz in the temperature range from 143 to 393 K. In order to minimize the amount of water in the samples and to avoid a change in water content during the experiment, the samples were initially held at 393 K for 1 h, and the measurements were performed during subsequent cooling under a flow of dry N $_2$ .

Dipolar relaxations were analyzed by fitting the dielectric loss  $\epsilon''$  or derivative spectra $^{21}$  using the appropriate form of the Havriliak–Negami equation

$$\epsilon''_{\text{HN}}(f) = \frac{\Delta\epsilon}{[1 + (iff_{\text{HN}})^a]^b} \quad (1)$$

for each relaxation process, where  $\Delta\epsilon$  is the relaxation strength,  $a$  and  $b$  are shape parameters, and  $f_{\text{HN}}$  is a characteristic frequency related to the frequency  $f_{\text{max}}$  of maximum loss by $^{22}$

$$f_{\text{max}} = f_{\text{HN}} \left( \sin \frac{a\pi}{2+2b} \right)^{1/a} \left( \sin \frac{ab\pi}{2+2b} \right)^{-1/b} \quad (2)$$

The analysis of conductivity and electrode polarization is described in section 3.3.

### 3. Results

**3.1. Characterization.** A single glass transition is obtained for both samples using differential scanning calorimetry, with

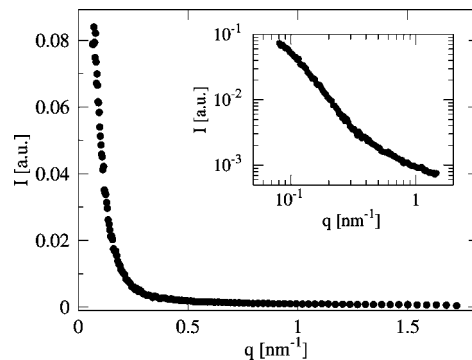


**Figure 2.** Small-angle X-ray scattering profile for PU $^-$ Na $^+$ .

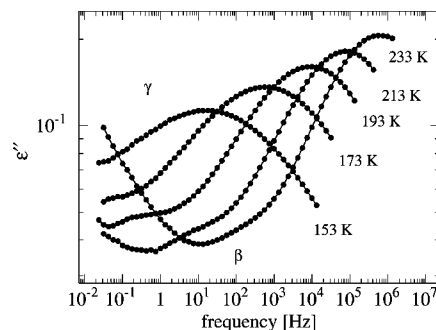


**Figure 3.** Dielectric loss vs frequency in the region of the secondary relaxations.

$T_g$  slightly higher (257 K) for PU $^-$ Na $^+$  than for PU $^-$ Li $^+$  (253 K). No crystallization of the samples is observed. These DSC results are consistent with those observed for polyester ionomers prepared from the same  $M_n = 600$  poly(ethylene glycol), $^{15,23}$  for which  $T_g = 258$  K for the Li ionomer and  $T_g = 267$  K for the Na ionomer.

Figure 2 shows the SAXS profile for PU $^-$ Na $^+$ . Considerable scattering is observed at low wavevectors; however, the scattering peak usually present for more conventional ionomers, $^{24,25}$  in which an appreciable portion of the polymer backbone is not polar, is not observed, indicating the absence of ion clusters. Similar low- $q$  scattering has been observed for polyester ionomers with a chemical structure closely related to the present samples $^{23}$  as well as for other ion-containing systems. $^{26,27}$  This scattering has been explained in terms of an inhomogeneous spatial distribution of ions, with regions of slightly different ion concentration having characteristic sizes of several tens of nanometers or more. As in the case of the PEO-containing sulfonated polyesters, $^{23}$  the strong interaction of ether oxygens with cations likely prevents microphase separation of ion clusters, and  $T_g$  far below room temperature allows equilibrium to be approximated.

**3.2. Molecular Mobility.** At temperatures below  $T_g$ , two dielectric loss peaks are observed which correspond to two secondary relaxation processes labeled  $\beta$  and  $\beta^*$  (Figure 3). Both  $\beta$  and  $\beta^*$  relaxation frequencies follow Arrhenius temperature dependences (Figure 5), with activation energies of 39 and 53 kJ/mol for  $\beta$  and  $\beta^*$ , respectively, for both samples.

The frequency/temperature position and activation energy of the  $\beta$  relaxation are similar to those of the local relaxation of poly(ethylene oxide), assigned to local chain twisting motions. $^{28}$  This relaxation is therefore assigned to local chain twisting in the PEO segments of the polyurethane ionomers. The very weak  $\beta^*$  relaxation is slower, with a higher activation energy. A relaxation process in the region between the segmental and  $\beta$  relaxations has been observed in semicrystalline poly(ethylene oxide) as well as in amorphous PEO/PMMA blends, where it

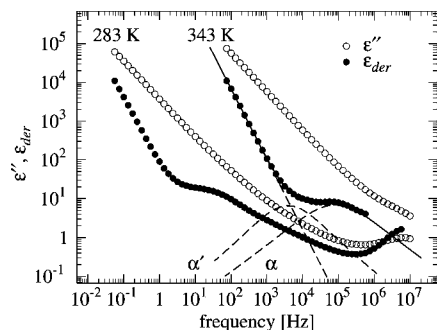


**Figure 4.** Dielectric loss (open symbols) and derivative (filled symbols) spectra at 283 and 343 K for PU-Na<sup>+</sup>. Lines are fits of the (appropriately transformed) Havriliak–Negami function to the 343 K  $\epsilon'_{\text{der}}$  data (individual contributions shown as dashed lines).

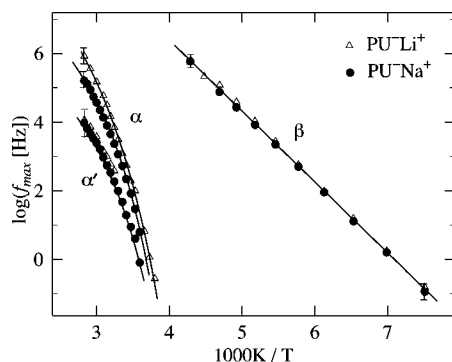


**Figure 5.** Peak frequency vs  $1/T$  for the  $\alpha$ ,  $\alpha'$ , and  $\beta$  relaxations.

was assigned to regions of partial crystalline order.<sup>29</sup> Alternatively, this process may be associated with motion of residual water molecules, remaining after drying, coupled with the local motion ( $\beta$  relaxation) of PEO segments.

At temperatures above  $T_g$ , the dielectric loss spectra are dominated by conductivity. Since the large values of the dielectric loss at low frequencies due to conduction/electrode polarization (EP) mask any loss peaks due to ionomer motion, the derivative formalism<sup>21</sup>

$$\epsilon'_{\text{der}}(f) = -\frac{2}{\pi} \frac{\partial \epsilon'(f)}{\partial \ln f} \quad (3)$$

was employed in order to resolve the dipolar processes in this temperature range (Figure 4).<sup>44</sup>

It was not possible to fit the derivative spectra with a single  $\alpha$  relaxation plus a power law; an additional relaxation slower than  $\alpha$ , noted as  $\alpha'$ , is needed to obtain an acceptable fit. The second, low-frequency relaxation is evident in the spectra only at high temperatures as a change in slope. Whether  $\alpha'$  is a separate relaxation or simply a pronounced low-frequency broadening of the  $\alpha$  relaxation is not clear. Here we adopt the standard interpretation that since the relaxation is too broad to be described by a single Havriliak–Negami function, we use two functions,  $\alpha$  and  $\alpha'$ .

The frequencies of both the  $\alpha$  and  $\alpha'$  relaxations (Figure 5) follow VFT temperature dependences. The  $\alpha$  relaxation, assigned to the segmental relaxation related to the glass transition, is slightly slower for PU-Na<sup>+</sup> than for PU-Li<sup>+</sup>, in accordance with the difference in calorimetric  $T_g$ . The origin of the  $\alpha'$  relaxation however is not clear. It likely includes contributions from localized ion motion,<sup>30</sup> given the large combined dielectric strength of the  $\alpha$  and  $\alpha'$  relaxations (see discussion of the static dielectric constant in a later section). A second, slowed-down segmental relaxation of PEO segments coordinated with cations,

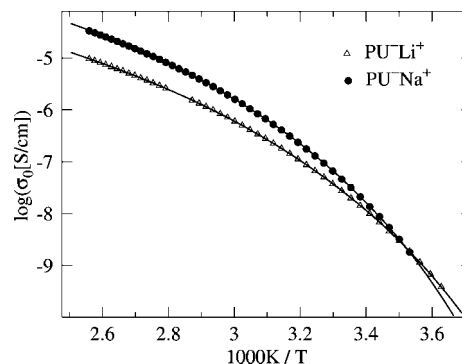


**Figure 6.** Dc conductivity vs inverse temperature. Uncertainty is comparable to the size of the data points.

such as that observed by molecular dynamics simulations,<sup>31</sup> may also contribute to the  $\alpha'$  process.

**3.3. Conductivity.** *Conductivity and Electrode Polarization.* Figure 6 displays dc conductivity as determined by fitting the linear portion of the dielectric loss curves in the low-frequency region using

$$\epsilon''(f) = \frac{\sigma_0}{2\pi f \epsilon_0} \quad (4)$$

The dependence of the conductivity on temperature can be fit using a VFT equation. Vogel temperatures for the conductivity ( $T_{0,\sigma} = 214 \pm 5$  and  $215 \pm 5$  K for Na and Li ionomers, respectively) are close to those for the relaxation times of the  $\alpha$  ( $T_{0,\alpha} = 207 \pm 5$  and  $194 \pm 5$  K) and  $\alpha'$  ( $T_{0,\alpha'} = 207 \pm 10$  and  $202 \pm 10$  K) processes, indicating that the conduction process is controlled by the segmental motions of the polymer chains. However, the physical significance of such an analysis is questionable since it ignores the possibility of the number of mobile charge carriers changing with temperature.<sup>15</sup>

The conductivity can be separated into the contributions of mobile ion concentration and ion mobility using a physical model for electrode polarization.<sup>15,32,33</sup> When applying a low-frequency field across blocking electrodes, and assuming that diffusing ions do not strongly interfere with each other, the contribution of electrode polarization to the complex dielectric function can be modeled as a macroscopic Debye relaxation:

$$\epsilon_{\text{EP}}^*(f) = \frac{\Delta \epsilon_{\text{EP}}}{1 + i2\pi f \tau_{\text{EP}}} \quad (5)$$

with an apparent relaxation time of

$$\tau_{\text{EP}} = \frac{L}{2L_D} \frac{\epsilon_s \epsilon_0}{q\mu p} \quad (6)$$

and apparent dielectric increment

$$\Delta \epsilon_{\text{EP}} = \left( \frac{L}{2L_D} - 1 \right) \epsilon_s \quad (7)$$

where

$$L_D = \frac{1}{q} \left( \frac{\epsilon_s \epsilon_0 kT}{p} \right)^{1/2} \quad (8)$$

is the Debye length,  $p$  the free ion concentration,  $\mu$  the ion mobility, and  $\epsilon_s$  the static dielectric constant. In the presence of electrode polarization, expression 5 replaces the usual dc conductivity contribution of eq 4. Equation 5 may be used to simultaneously fit  $\epsilon'(f)$  and  $\epsilon''(f)$  spectra, giving  $p$ ,  $\mu$ , and  $\epsilon_s$  directly as fitting parameters.

In terms of an equivalent circuit, eq 5 corresponds to a capacitor with capacitance  $C = \epsilon_0 \Delta \epsilon_{\text{EP}}$ , per unit area, inserted

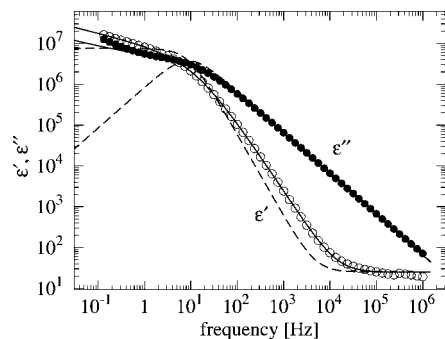


**Figure 7.** Dielectric constant and loss vs frequency at 393 K for PU-Na<sup>+</sup>. At this temperature the segmental relaxation is outside the frequency range of the measurement. Lines are fits of eqs 5 (dashed line) and 9 (solid lines) to the data.

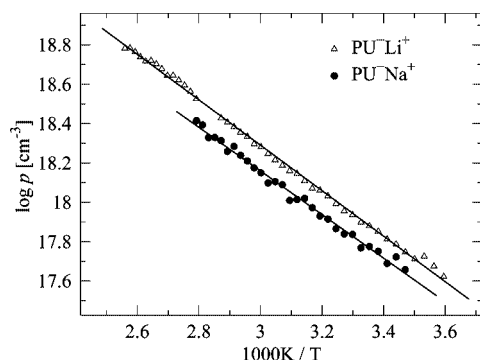


**Figure 8.** Number density of mobile ions vs inverse temperature for PU-Na<sup>+</sup> and PU-Li<sup>+</sup>. Lines are fits of eq 10 to the data, with  $E_a = 22$  kJ/mol.

in series with the sample, representing the impedance of the sample–electrode interface.<sup>32</sup> It has been found, however, that in practice electrode polarization is more accurately modeled with a constant phase element, with impedance  $Z \propto (i\omega)^{-n}$ , where the exponent  $n$  has been connected with electrode roughness.<sup>34–36</sup> By analogy with eq 5, the contribution of electrode polarization can now be written as

$$\varepsilon_{\text{EP,CPE}}^*(f) = \frac{\Delta\varepsilon_{\text{EP}}}{(i2\pi f\tau_{\text{EP}})^{1-n} + i2\pi f\tau_{\text{EP}}} \quad (9)$$

Fits of eqs 5 and 9 to typical  $\varepsilon'(f)$  and  $\varepsilon''(f)$  spectra for the polyurethane ionomers are shown in Figure 7. The modified eq 9 provides much better fits to the data, reproducing the shape of the curves over the entire frequency range, whereas eq 5 cannot describe the shape of the peak at frequencies lower than that of the EP peak,  $f < 1/(2\pi\tau_{\text{EP}})$ . Values of  $p$ ,  $\mu$ , and  $\varepsilon_s$  obtained using the two equations were similar, and the results discussed below were obtained using eq 9. Values of the parameter  $n$  were  $\sim 0.85$ – $0.90$ , as expected for nominally (but not molecularly) smooth brass electrodes. Note that at frequencies  $f \gg 1/(2\pi\tau_{\text{EP}})$  the dielectric loss vs frequency calculated from both eqs 5 and 9 takes the form of a power law with slope  $-1$ , and this analysis is consistent with using eq 4 in this frequency range to determine conductivity.

**Mobile Ion Concentration.** Figure 8 shows the mobile ion concentration determined using the EP model. Similar values are obtained for PU-Li<sup>+</sup> and PU-Na<sup>+</sup>. The value of mobile ion concentration is surprisingly low, with less than 0.1% of the ions being mobile at room temperature ( $T > T_g$ ). The temperature dependence of the mobile ion concentration is well described by an Arrhenius equation

$$p = p_\infty \exp(-E_a/kT) \quad (10)$$

where  $p_\infty$  is the mobile ion concentration as  $T \rightarrow \infty$  and  $E_a$  an activation energy. The pre-exponential factor  $p_\infty$  is  $\sim 10^{21}$  cm<sup>-3</sup>

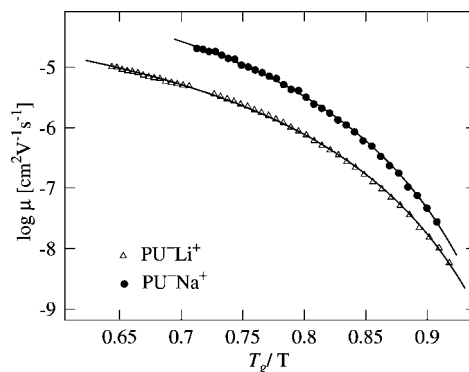


**Figure 9.** Ion mobility vs inverse temperature. Lines are fits of eq 11 to the data.

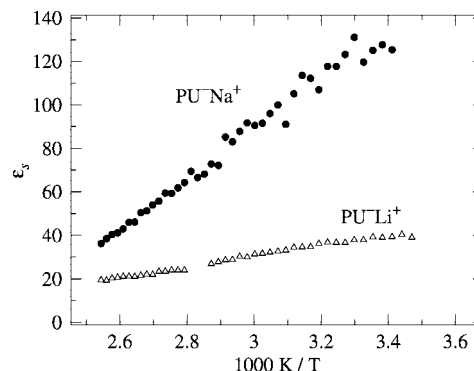


**Figure 10.** Static dielectric constant, determined from the EP model, vs inverse temperature.

for both ionomers and is within an order of magnitude of the total ion concentration determined from the stoichiometry ( $3 \times 10^{20}$  cm<sup>-3</sup>). The activation energy is  $E_a = 22$  kJ/mol for both PU-Li<sup>+</sup> and PU-Na<sup>+</sup>. Both the small values of mobile ion concentration as well as the Arrhenius temperature dependence agree with previous results obtained using the EP model on various PEO-based single-ion conductors and polymer–salt mixtures.<sup>15–17</sup>

**Ion Mobility.** The ion mobility determined from the EP model is displayed in Figure 9 vs inverse temperature. The data are well described by a Vogel–Fulcher–Tammann (VFT) equation

$$\mu = \mu_\infty \exp\left(-\frac{B_\mu}{T - T_{0,\mu}}\right) \quad (11)$$

where  $\mu_\infty$  is the ion mobility as  $T \rightarrow \infty$ ,  $B$  a constant, and  $T_0$  the Vogel temperature, at which mobility goes to zero. The VFT temperature dependence of ion mobility reflects the coupling of ion motion to polymer segmental mobility. To enable the comparison of the mobilities for the two ionomers, the values are plotted against  $T_g/T$  in Figure 9 to account for the difference in  $T_g$  between the two samples. The data do not collapse onto a single curve; instead, Na ions have somewhat higher mobility than Li ions for the same  $T - T_g$ . Very similar results were also obtained for PEO-based polyester ionomers,<sup>15</sup> where Li<sup>+</sup> ions were found to have lower mobility, at the same  $T_g/T$ , than Na<sup>+</sup> or Cs<sup>+</sup> ions. The lower ion mobility in PU-Li<sup>+</sup> may be understood in terms of the lower binding energy of the larger Na ions to the ether oxygens compared to the Li ions (observed for model systems such as dimethyl ether<sup>37</sup> and crown ethers),<sup>38</sup> which results in a lower energy barrier for cation motion.

**Static Dielectric Constant.** The static dielectric constant  $\varepsilon_s$ , a fitting parameter obtained from the EP model, is shown in Figure 10. The values of  $\varepsilon_s$  from EP model fitting agree with what is indicated by the experimental data (Figure 7) after subtraction of the electrode polarization. The dielectric constant



of our polymer without sulfonation or cations is expected to be on the order of 10–15, as polyesters with closely related chemical structures have  $\epsilon_s = 12$ . However,  $\epsilon_s$  for the ionomers is much higher, especially for PU- $\text{Na}^+$  where it reaches values of more than 100 at the lowest temperatures studied. Since  $\epsilon'$  has similar values of 3–5 for both PU- $\text{Na}^+$  and PU- $\text{Li}^+$  at frequencies above that of the segmental relaxation, the large dielectric constant  $\epsilon_s$  results from the large combined dielectric relaxation strength of the  $\alpha$  and  $\alpha'$  processes. Such large dielectric constants have been observed for other PEO-based ionomer systems<sup>15,16,45</sup> but, interestingly, not for polymer–salt mixtures of similar ion concentrations.<sup>16,30</sup> We therefore attribute the effect to bound ion pairs: such ion pairs constitute large dipoles which, in the case of ionomers, are attached to the polymer chain and participate in segmental motions, thus greatly increasing the dielectric strength of the segmental relaxations. The rapid decrease of  $\epsilon_s$  with increasing temperature reflects, then, the temperature dependences of  $\Delta\epsilon_\alpha$  and  $\Delta\epsilon_{\alpha'}$ .

The dielectric constant of the Na-containing ionomer is significantly larger than that of the Li variant, as reported for PEO-based polyester ionomers.<sup>15</sup> The reasons underlying this difference are unclear at present. Part of this effect can be accounted for by the larger ionic radius of the sodium ion; however, this difference is not sufficient to account for 3 times larger  $\epsilon_s$  values for PU- $\text{Na}^+$ . This suggests that there are ion-specific differences in the local environment of the bound ion pairs, especially in the coordination with neighboring ether oxygens, which result in a significantly smaller effective dipole moment for a sulfonate–lithium ion pair than for sulfonate–sodium pair.

#### 4. Discussion

In the previous discussion, we considered ion pairs but have neglected the possibility of larger ion aggregates, such as triple ions and quadrupoles. The existence of such aggregates has often been invoked to explain the concentration dependence of conductivity for polymer–salt systems, especially at high concentrations. Quadrupoles can reasonably be expected to form through the dipole–dipole interactions of neighboring ion pairs. In the case of ionomers, unlike polymer–salt systems, association of ion pairs into larger aggregates will not significantly affect conductivity, since both pairs and aggregates are immobile. However, note that quadrupoles, having no dipole moment, do not contribute to the increase of the static dielectric constant. As a result, an increased tendency for quadrupole formation in PU- $\text{Li}^+$  compared to PU- $\text{Na}^+$  could account for the difference in dielectric constant between the two ionomers, although it is not clear why such a tendency would be expected.

We now turn to the free ion concentration. The primary result obtained from the analysis of electrode polarization is that there is a very small fraction of free ions. Using the same EP model, tiny fractions of free ions were reported in previous studies of ion-containing polyether-based systems, both single-ion conductors (polyphosphazene-based ionomers,<sup>16</sup> PEO-based polyester ionomers)<sup>15</sup> and salt-containing polymer systems (polyphosphazene + LiTFSI,<sup>16</sup> PEO + LiClO<sub>4</sub>).<sup>17</sup> In all of the above systems the free ion concentration is very small (typically a fraction of 1% at  $T_g + 50$  K) and increases with increasing temperature following an Arrhenius temperature dependence, which implies full ion dissociation at infinite temperature. Ion association seems therefore to be driven by the electrostatic attraction between anion and cation, and the activation energy of the free ion concentration is identified with the energy needed to separate an ion pair.<sup>15</sup>

However, significantly different results are obtained using several other methods for determining free ion concentration. Raman<sup>10</sup> and infrared<sup>39</sup> spectroscopies examine ion association by probing the chemical environment of the ions. Measurements of the diffusion

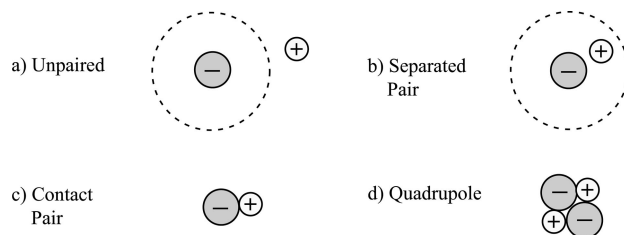


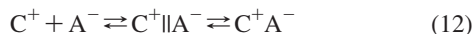
**Figure 11.** States of ion association. The dotted line indicates a distance of  $R$  (see text) from the anion. Only unpaired ions are detected as free using the EP model.

coefficient of anions and/or cations (by NMR<sup>11</sup> or radiotracer diffusion),<sup>14</sup> in combination with conductivity measurements, allow the determination of the degree of correlated ion motion, another measure of ion association. Both approaches typically report a significant free ion concentration that *decreases* with increasing temperature. This temperature dependence is also consistent with the phase separation (“salting out”) observed in certain polymer–salt complexes upon heating.<sup>2</sup> These results imply an entirely different physical picture for ion association: the driving force for ion association in polymer electrolytes is considered in this case to be entropic in nature due to the fact that, upon formation of an ion pair, polymer chain segments are released from coordination with the cation, thus increasing the number of available chain conformations.<sup>40</sup>

What is the origin of the discrepancy in the findings of the EP method, on one hand, and the spectroscopic and diffusion-based techniques, on the other? To answer this, one must specify more precisely what is meant by an ion pair in each case. In the case of the EP method, the free ion concentration is obtained through an indirect measurement of the Debye length (eq 5). Therefore, two ions are considered paired if they are close enough (closer than a certain distance  $R$ ) so as not to contribute to long-range ion interactions and not be counted in the calculation of the Debye length (Figure 11). In the context of theories of electrolyte solutions, various values for this distance  $R$  have been proposed, the usual choice being the Bjerrum length<sup>41</sup>  $l_B = q^2/(4\pi\epsilon_0\epsilon_s kT)$ . Ion pairs defined in this way include both *contact pairs* and *separated pairs*. Separated pairs have the cation separated from the anion by one or more polymer chains (referred to as solvent-separated or solvent-shared pairs in the terminology of electrolyte solutions).<sup>41,42</sup>

On the other hand, Raman and infrared spectroscopy are usually able to detect only contact ion pairs; in the case of separated pairs the perturbation of the vibrational states of the anion is usually too small to be detected. Both separated pairs and unpaired ions are thus “spectroscopically free”. Techniques based on measuring the diffusion coefficient of counterions also likely detect mainly contact pairs, at least in the case of radiotracer diffusion.<sup>13</sup> In molecular dynamics simulations, which find a large fraction of unpaired ions, pairs are specifically defined as contact pairs. The results obtained using the EP model may therefore be reconciled with those of the above techniques if a large fraction of the ions in the systems under investigation are in the form of separated pairs. These ions would be counted as free using vibrational and diffusion coefficient-based methods but as paired using the EP method.

The preceding explanation can also account for the different temperature dependence of the free ion concentration obtained by the different techniques. The critical difference between contact pairs and separated pairs lies in the fact that a cation in a separated pair is able to retain its preferred number of coordination bonds with the polymer chains, whereas to form a contact pair it is necessary to break a certain number of such bonds to accommodate the presence of the anion. The equilibrium among unpaired ions, separated pairs, and contact pairs can be written as



where  $C^+$  and  $A^-$  are cations and anions, respectively,  $C^+ \| A^-$  denotes a separated pair, and  $C^+ A^-$  denotes a contact pair. The temperature dependence observed by the EP method reflects the first equilibrium, while vibrational spectroscopy or diffusion-based methods observe the second. In the transition from free ions to a separated pair, the coordination of the cation to the polymer chain remains unchanged, and the main driving force for pair formation is electrostatic attraction. Conversely, an ion becomes unpaired (truly free) through a thermally activated process of fully overcoming electrostatic attraction. The concentration of unpaired ions will therefore increase with increasing temperature and an Arrhenius temperature dependence of the number of unpaired ions (as in eq 10) is reasonable. On the other hand, in the transition from a separated pair to a contact pair, the situation is more complicated: electrostatic attraction competes with the energetic cost of breaking cation–EO coordination bonds. In addition, there is an entropic effect due to the fact that upon contact pair formation the chain segments that are released from the cation have access to a greater number of conformations. This favors formation of contact pairs at high temperatures, and even potentially, phase separation as is in fact observed for salt-containing polymer systems.<sup>43</sup>

Returning to our polyurethane ionomers, the large difference in dielectric constant between PU–Li<sup>+</sup> and PU–Na<sup>+</sup>, even though the two ionomers have similar fractions of unpaired ions, can now be rationalized. Since Li<sup>+</sup> ions are more efficiently coordinated by the ether oxygens on the polymer chains compared to Na<sup>+</sup> ions, more contact pairs will be present in PU–Na<sup>+</sup>, leading to large values of the dielectric constant (Figure 10). The number of unpaired ions, however (Figure 8), is not affected, being controlled by electrostatic interactions which are identical for the two ionic species.

## 5. Summary

Molecular mobility and ionic transport in a series of model poly(ethylene oxide)-based polyurethane ionomers, containing mobile Li<sup>+</sup> or Na<sup>+</sup> were studied using dielectric relaxation spectroscopy. The ionomers are amorphous and exhibit a single calorimetric glass transition and no evidence of ion clustering in the small-angle X-ray scattering profile.

Two secondary relaxations were observed, which exhibit identical behavior for the ionomers containing Li<sup>+</sup> and Na<sup>+</sup> ions. In addition to the segmental  $\alpha$  relaxation, which is in good agreement with the calorimetric  $T_g$ , an additional slower relaxation is present, attributed either to localized ion motions or to the segmental relaxation process of PEO segments complexed with cations.

Using a physical model of electrode polarization, dc conductivity was decomposed into the contributions of free ion concentration and ion mobility. Very small values of free ion concentration are obtained, indicating a very large fraction of ions bound in ion pairs or larger aggregates. This result is rationalized, and reconciled with seemingly conflicting findings in the literature, using a model inspired by Fuoss,<sup>42</sup> where three ion states are considered: unpaired ions, separated pairs, and contact pairs.

**Acknowledgment.** The authors thank the Department of Energy, Office of Basic Energy Sciences, for support for this research through grant DE-FG02-07ER46409.

## References and Notes

- (1) Bruce, P. G.; Vincent, C. A. *J. Chem. Soc., Faraday Trans.* **1993**, *89*, 3187–3203.
- (2) Armand, M. *Solid State Ionics* **1994**, *69*, 309–319.
- (3) Meyer, W. H. *Adv. Mater.* **1998**, *10*, 439.
- (4) Wright, P. V. *MRS Bull.* **2002**, *27*, 597–602.
- (5) Borodin, O.; Smith, G. D. *Macromolecules* **2006**, *39*, 1620–1629.
- (6) Borodin, O.; Smith, G. D.; Geiculescu, O.; Creager, S. E.; Hallac, B.; DesMarteau, D. *J. Phys. Chem. B* **2006**, *110*, 24266–24274.
- (7) Duan, Y. H.; Halley, J. W.; Curtiss, L.; Redfern, P. *J. Chem. Phys.* **2005**, *122*, 8.
- (8) Kakihana, M.; Schantz, S.; Torell, L. M. *J. Chem. Phys.* **1990**, *92*, 6271–6277.
- (9) Salomon, M.; Xu, M. Z.; Eyring, E. M.; Petrucci, S. J. *Phys. Chem.* **1994**, *98*, 8234–8244.
- (10) Schantz, S. *J. Chem. Phys.* **1991**, *94*, 6296–6306.
- (11) Böhrer, R.; Jeffrey, K. R.; Vogel, M. *Prog. Nucl. Magn. Reson. Spectrosc.* **2007**, *50*, 87–174.
- (12) Obeidi, S.; Zazoum, B.; Stolwijk, N. A. *Solid State Ionics* **2004**, *173*, 77–82.
- (13) Stolwijk, N. A.; Obeidi, S. *Phys. Rev. Lett.* **2004**, *93*, 125901.
- (14) Stolwijk, N. A.; Wiencierz, M.; Obeidi, S. *Faraday Discuss.* **2007**, *134*, 157–169.
- (15) Klein, R. J.; Zhang, S. H.; Dou, S.; Jones, B. H.; Colby, R. H.; Runt, J. *J. Chem. Phys.* **2006**, *124*, 144903.
- (16) Klein, R. J.; Welna, D. T.; Weikel, A. L.; Allcock, H. R.; Runt, J. *Macromolecules* **2007**, *40*, 3990–3995.
- (17) Matsumiya, Y.; Balsara, N. P.; Kerr, J. B. *Macromolecules* **2004**, *37*, 7064–7064.
- (18) Polizos, G.; Georgoussis, G.; Kyritsis, A.; Shilov, V. V.; Shevchenko, V. V.; Gomza, Y. P.; Nesin, S. D.; Klimenko, N. S.; Wartewig, S.; Pissis, P. *Polym. Int.* **2000**, *49*, 987–992.
- (19) Polizos, G.; Kyritsis, A.; Pissis, P.; Shilov, V. V.; Shevchenko, V. V. *Solid State Ionics* **2000**, *136*, 1139–1146.
- (20) Pissis, P.; Polizos, G. In *Handbook of Condensation Thermoplastic Elastomers*; Fakirov, S., Ed.; Wiley-VCH: New York, 2005.
- (21) Wubbenhorst, M.; van Turnhout, J. *J. Non-Cryst. Solids* **2002**, *305*, 40–49.
- (22) *Broadband Dielectric Spectroscopy*; Kremer, F.; Schöhal, A., Eds.; Springer-Verlag: Berlin, 2002.
- (23) Dou, S.; Zhang, S.; Klein, R. J.; Runt, J.; Colby, R. H. *Chem. Mater.* **2006**, *18*, 4288–4295.
- (24) Yarusso, D. J.; Cooper, S. L. *Polymer* **1985**, *26*, 371–378.
- (25) Eisenberg, A.; Hird, B.; Moore, R. B. *Macromolecules* **1990**, *23*, 4098–4107.
- (26) Ding, Y. S.; Hubbard, S. R.; Hodgson, K. O.; Register, R. A.; Cooper, S. L. *Macromolecules* **1988**, *21*, 1698–1703.
- (27) Wu, D. Q.; Phillips, J. C.; Lundberg, R. D.; Macknight, W. J.; Chu, B. *Macromolecules* **1989**, *22*, 992–995.
- (28) Jin, X.; Zhang, S. H.; Runt, J. *Polymer* **2002**, *43*, 6247–6254.
- (29) Jin, X.; Zhang, S. H.; Runt, J. *Macromolecules* **2004**, *37*, 8110–8115.
- (30) Zhang, S. H.; Runt, J. *J. Phys. Chem. B* **2004**, *108*, 6295–6302.
- (31) Borodin, O.; Smith, G. D. *Macromolecules* **2000**, *33*, 2273–2283.
- (32) Macdonald, J. R. *Phys. Rev.* **1953**, *92*, 4–17.
- (33) Coelho, R. *J. Non-Cryst. Solids* **1991**, *131*, 1136–1139.
- (34) Brug, G. J.; Vandeneeden, A. L. G.; Sluytersrehabach, M.; Sluyters, J. H. *J. Electroanal. Chem.* **1984**, *176*, 275–295.
- (35) Pajkossy, T. *Solid State Ionics* **2005**, *176*, 1997–2003.
- (36) Bordin, F.; Cametti, C.; Colby, R. H. *J. Phys.: Condens. Matter* **2004**, *16*, R1423–R1463.
- (37) Hill, S. E.; Glendening, E. D.; Feller, D. *J. Phys. Chem. A* **1997**, *101*, 6125–6131.
- (38) Hill, S. E.; Feller, D.; Glendening, E. D. *J. Phys. Chem. A* **1998**, *102*, 3813–3819.
- (39) Guha, C.; Chakraborty, J. M.; Karanjai, S.; Das, B. *J. Phys. Chem. B* **2003**, *107*, 12814–12819.
- (40) Ratner, M. A.; Nitzan, A. *Faraday Discuss. Chem. Soc.* **1989**, *88*, 19–42.
- (41) Marcus, Y.; Hefter, G. *Chem. Rev.* **2006**, *106*, 4585–4621.
- (42) Fuoss, R. M. *J. Phys. Chem.* **1978**, *82*, 2427–2440.
- (43) Mehta, M. A.; Lightfoot, P.; Bruce, P. G. *Chem. Mater.* **1993**, *5*, 1338–1343.
- (44) The derivative formalism is typically used, in the absence of electrode polarization and for relatively broad loss peaks, as a good approximation to “ohmic conduction-free” dielectric loss. In the presence of electrode polarization, the EP peak observed in the dielectric loss has a corresponding contribution to  $\epsilon'$ ; therefore, it is also present as a peak in the derivative spectrum. However, the width of the EP peak is considerably reduced in the  $\epsilon''(f)$  spectrum compared to the corresponding peak in  $\epsilon'(f)$ , allowing the dipolar processes present at higher frequencies to be resolved.
- (45) The downturn of  $\epsilon_s$  at low temperatures previously reported for PEO-based polyester ionomers<sup>15</sup> is an artifact, appearing at temperatures where the segmental relaxation is partially outside the frequency window of the dielectric measurements.